J Therm Anal Calorim (2010) 99:399–407
DOI 10.1007/s10973-009-0130-4

Crystallization and melting behavior of PP/nano-$CaCO_3$ composites with different interfacial interaction

Yuhai Wang · Hao Shen · Gu Li · Kancheng Mai

Received: 23 February 2009 / Accepted: 3 April 2009 / Published online: 13 August 2009

Abstract The effect of different interfacial interaction on the crystallization and melting behavior of PP/nano-$CaCO_3$ composites was investigated using differential scanning calorimetry, X-ray diffraction and polarized optical microscope. The results indicated that nano-$CaCO_3$ acted as heterogeneous nuclei for PP crystallization. There existed a synergistic effect of heterogeneous nucleation between nano-$CaCO_3$ and compatibilizer for PP crystallization, which was proved by increasing the crystallization rate and decreasing the fold surface free energy as well as favoring the formation of β-crystal of PP. However, this synergistic effect was dependent on the interfacial interaction between PP and compatibilizer. The increased miscibility between compatibilizer and PP favored this synergistic effect.

Keywords Compatibilizer · Crystallization · Interfacial interaction · Polypropylene

Introduction

Recently, polymer nanocomposites became a subject of many studies and applications because it is believed that the tremendous interfacial area between nanoparticles and polymer helps to influence the composite's properties to a great extent [1]. Many studies have shown that polypropylene (PP) nanocomposites exhibited enhanced strength, toughness, heat distortion temperatures, flame resistance, barrier properties and decreased thermal expansion coefficient [2–8]. Of these nanocomposites, PP/$CaCO_3$ nanocomposites have attracted considerable interests because of the availability of nano-$CaCO_3$ in readily usable form and low cost. Therefore, PP composites filled by nano-$CaCO_3$ have been extensively studied [9–22]. Yang et al. [12] reported that nano-$CaCO_3$ particles had better toughening effect on improving the impact strength of PP matrix than micro-$CaCO_3$ particles. Weon et al. [13] reported that addition of nano-$CaCO_3$ reduced the size of spherulites of PP and induced the formation of β-phase crystallites, which led to a more ductile PP matrix and improved the impact strength of PP. Similar result was observed by Mai et al. [11]. Chan et al. [14] also found that nano-$CaCO_3$ particle was a very effective nucleating agent for PP.

However, nanoparticles tend to agglomerate in the polymer matrix due to the tremendous surface area and high surface free energy. Aggregation has a detrimental effect on the properties of polymer composites [10, 15]. In order to improve the dispersion of the nanoparticles, the coupling agents (e.g. silane and titanate) and macromolecular compatibilizers were used to modify the surface of the particles. Surface treatment changes the interfacial interaction between particles and polymer matrix, and then influences the crystallization and melting behavior of polymer composites. It is found that nano-$CaCO_3$ particles treated with nonionic modifier increased the crystallization rate of PP matrix [11]. Similar result was obtained when surface modified with a coupling agent [22]. However, a contrary result was found by Avella et al. [16] that addition of nano-$CaCO_3$ coated with fatty acids delays crystallization of PP. Avella et al. [16, 17] also demonstrated that addition of PP-g-MA enhanced the heterogeneous nucleation ability of nano-$CaCO_3$ particles by improving the

Y. Wang · H. Shen · G. Li · K. Mai (✉)
Key Laboratory of Polymeric Composites and Functional Materials, the Ministry of Education, Materials Science Institute, School of Chemistry and Chemical Engineering, Sun Yat-sen University, Guangzhou 510275, People's Republic of China
e-mail: cesmkc@mail.sysu.edu.cn

interfacial interaction between $CaCO_3$ particles and PP. Mai et al. [20] found that the PP-g-AA could improve the heterogeneous nucleation effect of nano-$CaCO_3$ and further increased the crystallization temperature of PP. Surface treatment also influence the mechanical properties of PP/nano-$CaCO_3$ composites. Mai et al. [11] found the addition of a nonionic modifier greatly improved the Izod impact energy of PP/$CaCO_3$ nanocomposites due to lowering the particle–polymer interaction. Ma et al. [21] demonstrated that an obvious synergistic effect between the grafted PBA and nano-$CaCO_3$ led to a significant increment in notched impact strength duo to the chemical bonding between the elastomer grafted PBA and nano-$CaCO_3$.

Many investigations indicated that the interfacial interaction among polymer composites plays an important role in determining the physical and mechanical properties of polymer composites. Thus, the study on the relationship between the interfacial interaction and the properties of polymer composite is of great importance. Although polymer composites with desired structures and properties can be obtained by selecting appropriate surface treatment agent or macromolecular compatibilizer to control the interfacial interaction between inorganic particles and polymer matrix, the surface treatment agent, including low molecule surfactants and macromolecular compatibilizer, was generally considered as a whole interface in many investigations. In fact, when modified by polar macromolecular compatibilizer, a core-shell structure with particles encapsulated by compatibilizer would be formed in polymer matrix, resulting in the formation of two interfaces: the interface between particles and compatibilizer as well as the interface between compatibilizer and polymer matrix. Few studies have done to investigate the effect of these two interfaces on the properties of PP composites [23].

In order to investigate the effect of interfacial interaction on the crystallization behavior of PP/nano-$CaCO_3$ composites, three kinds of compatibilizers (PP-g-MA, POE-g-MA and EVA-g-MA) with the same polar groups (MA) but different backbones were used as compatibilizers to obtain the different interfacial interactions. It is believed that the MA polar group of compatibilizers would associate with the surface of nano-$CaCO_3$ particles by polarity–polarity interaction, resulting in the formation of the similar interfacial interaction between nano-$CaCO_3$ particles and compatibilizers. The different miscibility between the macromolecular chain of compatibilizer and PP matrix results in the formation of different interfacial interaction between PP matrix and compatibilizer. The effect of interfacial interaction between PP matrix and compatibilizer on the crystallization and melting behavior as well as morphology of PP/nano-$CaCO_3$ composites was investigated in this paper.

Experimental

Materials

Polypropylene (EPS30R), ethylene content 2.87%, MFI = 2.1 g/10 min (2.16 kg at 230 °C), was supplied by Dushanzi Petroleum Chemical, China. Polypropylene grafted with maleic anhydride (PP-g-MA), grafting ratio 1.0%, MFI > 15 g/10 min (2.16 kg at 230 °C); Ethylene–octene copolymer grafted with maleic anhydride (POE-g-MA), grafting ratio 1.1%, MFI = 0.72 g/10 min (2.16 kg at 230 °C); Ethylene–vinyl acetate copolymer grafted with maleic anhydride (EVA-g-MA), grafting ratio 1.0%, MFI = 2.46 g/10 min (2.16 kg at 230 °C). The compatibilizers were provided by Guangzhou Lushan Chemical Materials Co. China. Nano-$CaCO_3$ (CC), with particle size of 70–90 nm was obtained from Shiraishi Kogyo Kaisha LTD, Japan.

Sample preparation

All materials were dried in an oven at 60 °C for 12 h. PP/nano-$CaCO_3$ composites with and without compatibilizers were prepared using a Berstoff ZE25A corotating twin-screw extruder. The blending temperature was set at 200 °C. All the materials were simultaneously added into the extruder after previous mixing. The compositions for the specimens are listed in Table 1.

Methods

The crystallization behavior of specimens was examined using Perkin–Elmer DSC-7 differential scanning calorimetry (DSC) under nitrogen atmosphere. The heat flow and temperatures of DSC were calibrated with standard materials, indium and zinc. The weight of specimens is about 5 mg. For non-isothermal crystallization, the specimens were rapidly heated to 220 °C at a rate of 200 °C/min and melted for 3 min to erase the thermal history, and then cooled down to 50 °C at a rate of 10 °C/min. The crystallized specimens were re-heated at a rate of 10 °C/min to investigate the melting behavior of PP. For isothermal crystallization, all the specimens were heated to 220 °C at a rate of 200 °C/min and melted for 3 min, and then rapidly cooled down at a rate of 200 °C/min to different designed crystallization temperatures (T_c) for 30 min. The crystallized specimens were heated at rate of 10 °C/min to investigate the corresponding melting behavior of PP.

A Rigaku D/max-2200 VPC X-ray diffractometer with the Cu Kα radiation at a voltage of 40 kV and a current of 30 mA was used for Wide angle X-ray diffraction (WAXD) experiments. The scan speed was 4°/min in a range of 2θ = 5–40° at ambient temperature. The specimens were

Table 1 The compositions for PP/nano-$CaCO_3$ composites

Samples	PP/wt%	$CaCO_3$/wt%	PP-g-MA/wt%	POE-g-MA/wt%	EVA-g-MA/wt%
PP	100	–	–	–	–
PP-a	95	–	5	–	–
PP-b	95	–	–	5	–
PP-c	95	–	–	–	5
CC-a	–	67	33	–	–
CC-b	–	67	–	33	–
CC-c	–	67	–	–	33
PP-5	95	5	–	–	–
PP-10	90	10	–	–	–
PP-15	85	15	–	–	–
PP-20	80	20	–	–	–
PP-10a	85	10	5	–	–
PP-10b	85	10	–	5	–
PP-10c	85	10	–	–	5

pre-treated on Perkin–Elmer DSC-7 thermal system, heating rapidly to 220 °C, holding for 3 min, and then cooling to 50 °C at rate of 10 °C/min.

The spherulitic morphology of specimens was observed with a LEIT2, Orthoplan Pol polarized optical microscope (POM) equipped with a crossed polarizer and a hot stage. The ~10 μm thick films cut perpendicularly to the injection molding direction of the rectangular bars and was melted at 200 °C for 3 min via the hot stage, and then the specimen was cooled down to room temperature at a rate of 10 °C/min.

Results and discussion

Non-isothermal crystallization and melting behavior of PP/nano-$CaCO_3$ composites

Figure 1 shows non-isothermal crystallization and melting curves of PP and PP/nano-$CaCO_3$ composites, the crystallization and melting parameters are listed in Table 2. It can be seen that a small amount of nano-$CaCO_3$ can increase the crystallization temperature (T_c) of PP about 3–4 °C due to the heterogeneous nucleation of nano-$CaCO_3$. Many other nanopaticles were also found to have nucleation effect for PP crystallization [24, 25]. However, the T_c of PP changed little with increasing nano-$CaCO_3$ content. It is suggested that there would be a saturated content for the heterogeneous nucleation of nano-$CaCO_3$ for PP crystallization in PP/nano-$CaCO_3$ composites, just as demonstrated by Mai et al. [23, 26] in the study of the crystallization behavior of PP/$Mg(OH)_2$ composite. Addition of nano-$CaCO_3$ also causes a slight increase in the

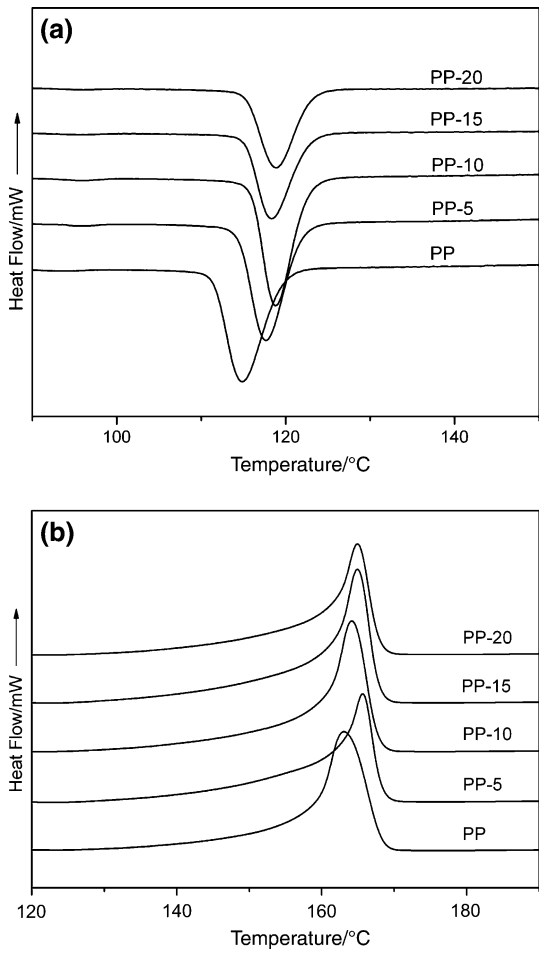

Fig. 1 DSC **a** crystallization and **b** melting curves of PP and PP/nano-$CaCO_3$ composites

Table 2 DSC results of non-isothermal crystallization and melting of PP/compatibilizer blends and PP/nano-$CaCO_3$ composites[a]

Samples	T_c/°C	T_c^{on}/°C	T_m/°C	T_m^{on}/°C	ΔH_c/J g^{-1}
PP	114.8	119.6	163.7	159.0	84.1
PP-g-MA	113.6	116.8	161.6	154.6	86.5
POE-g-MA	43.3	46.4	61.1	24.2	17.6
EVA-g-MA	70.2	75.6	89.4	65.1	14.8
PP-a	116.2	120.1	163.6	158.2	85.3
PP-b	113.5	117.4	162.7	157.3	83.5
PP-c	112.6	115.0	162.4	157.0	83.0
CC-a	117.8	122.4	160.0	155.1	86.1
CC-b	42.9	46.3	61.4	20.1	18.3
CC-c	71.9	77.4	88.9	64.9	16.3
PP-5	117.7	121.9	165.0	160.0	83.5
PP-10	118.8	122.6	164.4	160.5	83.6
PP-15	118.4	122.6	164.8	160.9	82.0
PP-20	118.9	123.0	164.9	160.4	82.9
PP-10a	123.0	126.6	165.5	160.8	86.1
PP-10b	119.9	123.6	164.7	160.6	87.5
PP-10c	114.1	118.4	163.6	158.8	84.0

[a] T_c, the peak crystallization temperature; T_c^{on}, the onset crystallization temperature; T_m, the peak melting temperature; T_m^{on}, the onset melting temperature; ΔH_c, the crystallization enthalpy, normalized by PP content

melting temperature of PP, which indicates the formation of more perfect crystal of PP. Mai et al. [18] found that nano-$CaCO_3$ could induce PP to form β-crystal and there was a melting peak of β-crystal at about 150 °C. However, there are no melting peaks at about 150 °C in the melting curves of PP/nano-$CaCO_3$ composites (Fig. 1b), indicating that nano-$CaCO_3$ could not induce the formation of β-crystal of PP in this study.

Non-isothermal crystallization and melting behavior of PP/compatibilizer blends

Three compatibilizers (PP-g-MA, POE-g-MA and EVA-g-MA) with the same polar grafted groups (MA) but different backbones were used to modify PP/nano-$CaCO_3$ composites. The crystallization and melting parameters of these compatibilizers are listed in Table 2. The crystallization temperature (T_c), melting temperature (T_m) and crystallization enthalpy (ΔH_c) of PP-g-MA are close to those of PP matrix. POE-g-MA and EVA-g-MA can also crystallize, however, the T_c, T_m and ΔH_c of POE-g-MA and EVA-g-MA are much lower than those of PP matrix.

Figure 2 shows the non-isothermal crystallization and melting curves of PP/compatibilizer blends, the crystallization and melting parameters are listed in Table 2. It can be observed from Fig. 2 and Table 2 that different compatibilizer has different influence on the crystallization

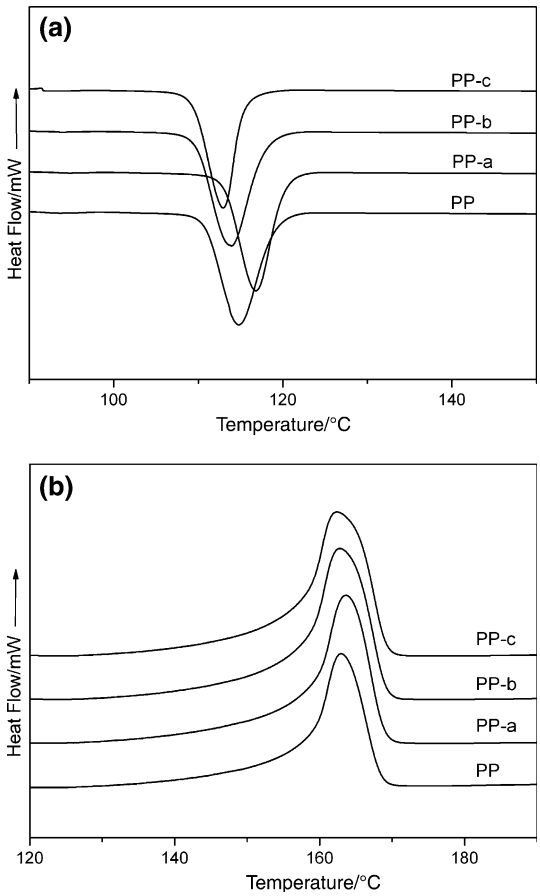

Fig. 2 DSC **a** crystallization and **b** melting curves of PP and PP/compatibilizer blends

behavior of PP matrix. Although the T_c of PP-g-MA is lower than that of PP, addition of PP-g-MA slightly increases the T_c of PP matrix. However, addition of POE-g-MA and EVA-g-MA with low T_c decreases the T_c of PP matrix. The increase of T_c of PP by adding PP-g-MA indicates that the compatibilizer has a heterogeneous nucleation for PP crystallization [27]. However, these heterogeneous nuclei formed by the heterogeneous nucleation of compatibilizer are located in the phase of compatibilizer. As a result, the heterogeneous nucleation of these heterogeneous nuclei in the phase of compatibilizer depends on the miscibility between compatibilizer and PP matrix.

Although the miscibility of PP-MA with PP generally decreases with the increase of MA content in the copolymer [28, 29], the PP chains in PP-g-MA are high miscible with PP matrix. Therefore the heterogeneous nucleation of the heterogeneous nuclei in PP-g-MA can induce the crystallization of PP matrix and increase the T_c of PP matrix. However, the POE chain in POE-g-MA is partially miscible with PP matrix [30] and the EVA chain in the EVA-g-MA is considered immiscible with PP matrix due

to the strong polar acetate group [31]. The decreased miscibility between compatibilizer and PP matrix restricts the heterogeneous nucleation of the heterogeneous nuclei in the phase of POE-g-MA or EVA-g-MA for PP crystallization. Furthermore, the partially miscible and/or immiscible components may disturb the crystallization of PP matrix [32]. Thus, the T_c of PP matrix in PP/POE-g-MA or EVA-g-MA blends is lower than that of neat PP.

Non-isothermal crystallization and melting behavior of PP/nano-$CaCO_3$ composites modified by compatibilizers

The non-isothermal crystallization and melting curves of PP in PP/nano-$CaCO_3$ composites modified by different compatibilizer are shown in Fig. 3. Table 2 gives the crystallization and melting parameters of these modified PP/nano-$CaCO_3$ composites. It can be observed from Fig. 3 and Table 2 that addition of PP-g-MA significantly increases the T_c of PP in PP/nano-$CaCO_3$ composites. The T_c of PP in PP-10a is approximately 8 °C higher than that of PP and 4 °C higher than that in PP-10. Addition of POE-g-MA slightly increases the T_c of PP in PP/nano-$CaCO_3$ composite, the T_c of PP-10b is about 5 °C higher than that of PP and 1 °C higher than that in PP-10. However, addition of EVA-g-MA reduces the T_c of PP in PP/nano-$CaCO_3$ composite and the T_c of PP-10c is even lower than that of PP.

When the compatibilizer is added into the PP/nano-$CaCO_3$ composite, nano-$CaCO_3$ particles will be encapsulated by compatibilizer due to the strong polar interaction between nano-$CaCO_3$ particles and compatibilizer, resulting in the formation of compatibilizer phase between nano-$CaCO_3$ and PP matrix. Two kinds of interface were formed: the interface between PP and compatibilizer, as well as the interface between particles and compatibilizer. Addition of PP-g-MA and POE-g-MA increases the T_c of PP in PP/nano-$CaCO_3$ composites, indicating that there exist a synergism of heterogeneous nucleation in the interface between compatibilizer and nano-$CaCO_3$ for PP crystallization. It is suggested that the chemical reaction between the polar groups (MA) of compatibilizer and nano-$CaCO_3$ particles in the interface between compatibilizer and nano-$CaCO_3$ results in the formation of carboxylate salts [33]. The carboxylate salts is a more effective nucleating agent than nano-$CaCO_3$ particle. Therefore, addition of compatibilizer increases the T_c of PP in PP/nano-$CaCO_3$ composites.

The heterogeneous nucleation of carboxylate salts not only increases the T_c of PP, but also induces the formation of β-crystal of PP. The peak at about 150 °C in Fig. 3b is attributed to the melting of β-crystal of PP. The β-crystal of PP is obtained for PP-10a and PP-10b with higher T_c of PP. However, no β-crystal of PP was formed in PP, PP-10 and PP-10c with lower T_c. The formation of β-crystal of PP is proved by WAXD measurement in Fig. 4. For PP-10a and

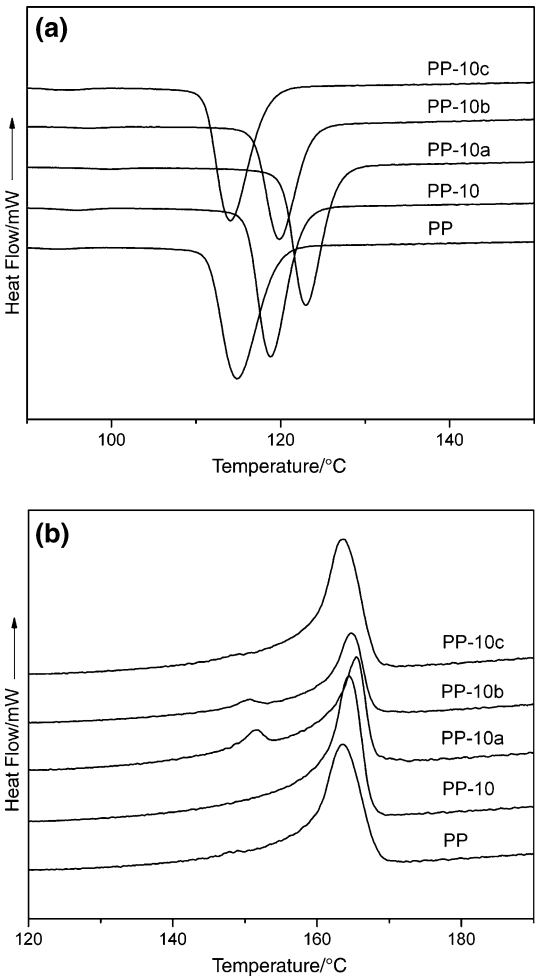

Fig. 3 DSC **a** crystallization and **b** melting curves of PP and PP/nano-$CaCO_3$ composites with and without compatibilizers

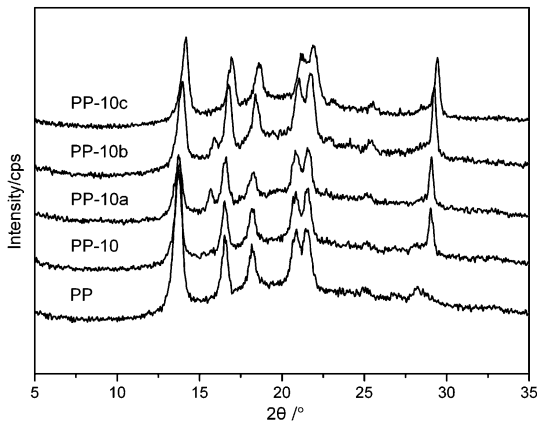

Fig. 4 WAXD patterns of PP and PP/nano-$CaCO_3$ composites with and without compatibilizers

PP-10b, a peak at $2\theta \approx 16°$ corresponding to β-crystal of PP is observed except for the characteristic crystalline peaks of α-crystal of PP. The synergism of heterogeneous nucleation in the interface between compatibilizers and nano-$CaCO_3$ for PP crystallization is also proved by optical micrographs in Fig. 5. Addition of nano-$CaCO_3$ particles dramatically increases the number of spherulites and decreases the size of spherulites due to the heterogeneous nucleation of nano-$CaCO_3$ particles. Addition of PP-g-MA or POE-g-MA further decreases the size of PP spherulites, and β-crystals of PP are visible in the optical micrographs of PP-10a and PP-10b (Fig. 5c, d). It is attributed to the heterogeneous nucleation of carboxylate salts between compatibilizers and nano-$CaCO_3$ particles.

Because of compatibilizer with the same polar groups, it is considered the interfacial interaction is basically same between nano-$CaCO_3$ and compatibilizer. Addition of EVA-g-MA decreases the T_c of PP and no β-crystal of PP are formed in PP-10c, and the spherulite size of PP in PP-10c is larger than that in PP-10. It is suggested that the heterogeneous nucleation of carboxylate salts is dependent on the miscibility between nano-$CaCO_3$ and compatibilizer. The carboxylate salts formed in the interface between nano-$CaCO_3$ particles and compatibilizer do not play a direct nucleation for PP crystallization due to the presence of the compatibilizer layer in the PP/nano-$CaCO_3$ composites. The heterogeneous nucleation of carboxylate salts may firstly nucleate the crystallization of compatibilizer layer and/or the PP matrix included in the compatibilizer phase, and then nucleates the PP matrix. Therefore, the heterogeneous nucleation of carboxylate salts depends on the crystallizability of compatibilizer and the miscibility between PP and compatibilizer.

It can be seen from Table 2 that addition of nano-$CaCO_3$ particles rarely affect the crystallization of POE-g-MA and EVA-g-MA, and slightly increase the T_c of PP-g-MA. The T_c of these three compatibilizers in compatibilizer/nano-$CaCO_3$ composites is lower than the T_c of PP matrix in the corresponding PP/compatibilizer/nano-$CaCO_3$ composites.

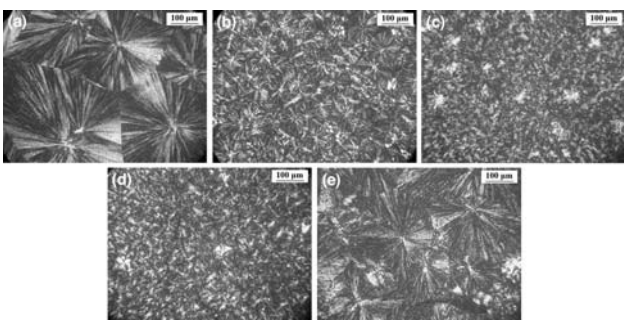

Fig. 5 POM photographs of PP and PP/nano-$CaCO_3$ composites with and without compatibilizers **a** PP, **b** PP-10, **c** PP-10a, **d** PP-10b and **e** PP-10c

That is to say, in PP/compatibilizer/nano-$CaCO_3$ composites, the crystallization of PP matrix starts earlier than that of compatibilizer. Because the crystallization of compatibilizers does not affect the crystallization of PP matrix, it is suggested that the carboxylate salts mainly nucleate the crystallization of PP matrix included in compatibilizer phase, and then nucleates PP matrix. However, the content of PP matrix included in this phase is dependent on the miscibility between PP and compatibilizer. For PP-10a, PP-g-MA is highly miscible with PP matrix, and the heterogeneous nucleation of carboxylate salts can nucleate the PP matrix included in PP-g-MA phase, and then nucleates PP matrix, leading to a high T_c of PP in PP-10a. For PP-10b, the partial miscible between PP and POE in POE-g-MA decreases the content of PP matrix included in POE-g-MA phase, which weakens the nucleation effect of carboxylate salts. For PP-10c, the immiscibility between PP and EVA-g-MA retards the heterogeneous nucleation of carboxylate salts due to the few content of PP matrix in EVA-g-MA phase. Therefore, addition of EVA-g-MA into PP/nano-$CaCO_3$ composite decreased the T_c of PP and the spherulite size of PP is larger than that of PP-10.

Isothermal crystallization and melting behavior of PP/nano-$CaCO_3$ composites modified by compatibilizers

The synergism of heterogeneous nucleation of PP-g-MA and nano-$CaCO_3$ for PP crystallization are proved by isothermal crystallization experiment. The relationship of reciprocal crystallization peak time (i.e. t_p^{-1}) versus T_c for PP and its composites is shown in Fig. 6. Generally, t_p^{-1} is proportional to the crystallization rate [34]. It can be observed that the crystallization rates of PP and its composites decrease with the increase of isothermal crystallization temperatures. When isothermally crystallized at the same temperature, the t_p^{-1} of the specimens ranges as: PP-10a > PP-10b > PP-10 >> PP $\geq$ PP-10c. That is to say, the crystallization rate of these specimens ranges as: PP-10a > PP-10b > PP-10 >> PP $\geq$ PP-10c. These results are in agreement with those of non-isothermal crystallization experiment and indicated the presence of the synergism of heterogeneous nucleation of PP-g-MA and nano-$CaCO_3$ for PP crystallization increases the crystallization rate of PP.

Crystallization activation energy and fold surface free energy of PP crystallization in PP/nano-$CaCO_3$ composites

It is well known that the crystallization of polymers is controlled by two factors: the dynamic factor, which is related to the effective activation energy for the transport of

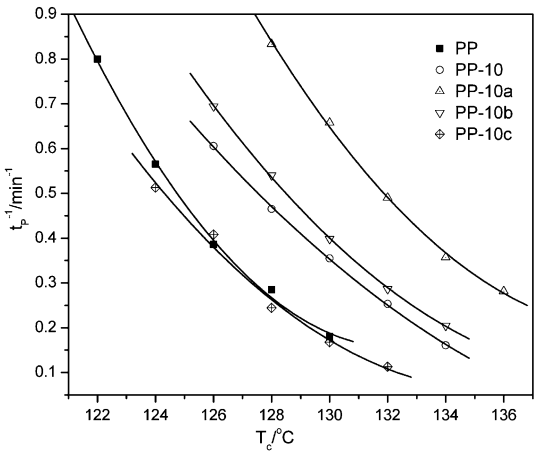

Fig. 6 The plots of reciprocal crystallization peak time (t_P^{-1}) against crystallization temperature for PP and PP/nano-$CaCO_3$ composites with and without compatibilizers

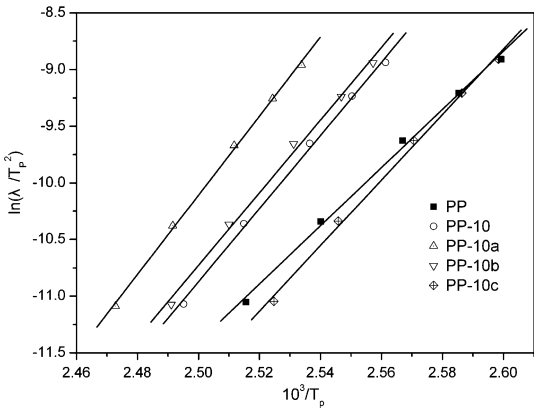

Fig. 7 The plots of $\ln(\lambda/T_p^2)$ against $1/T_p$ for PP and PP/nano-$CaCO_3$ composites with and without compatibilizers

crystalline unites across the phase, and the static factor, which is related to the free energy barrier for nucleation.

The activation energy (ΔE) in non-isothermal crystallization process can be determined by Kissinger method through calculating the variation of the crystallization peak temperature (T_p) with the cooling rate (λ) [35]:

$$\mathrm{d}\ln(\lambda/T_p^2)/\mathrm{d}(1/T_p) = -\Delta E/R \quad (1)$$

where R is the gas constant. Generally, high crystallization activation energy would hinder the crystallization and result in the decrease of crystallization rate.

The plots of $\ln(\lambda/T_p^2)$ against $1/T_p$ give a straight line (Fig. 7). The ΔE values of specimens can be calculated form the slope of the line, tabulated in Table 3. It can be seen that addition of nano-$CaCO_3$ increases the ΔE of PP. This result is similar to those reported for many other nucleating agents [36–38]. It is suggested that the addition of nano-$CaCO_3$ restricts the transport of macromolecular segments from PP melts to the crystal growth surface. The addition of PP-g-MA further increases the ΔE of PP in PP/nano-$CaCO_3$ composites due to the strong interaction between PP-g-MA and nano-$CaCO_3$ as well as good miscibility between PP-g-MA and PP matrix to restrict the transport of macromolecular segments of PP. The ΔE of modified composites decreases with decreasing the miscibility between compatibilizer and PP matrix.

According to the Hoffman theory, the growth rate G of crystals can be expressed as follows [39]:

$$G = G_0 \exp[-U^*/(R(T_c - T_\infty))]\exp[-K_g/(T_c\Delta T f)] \quad (2)$$

Assuming the growth rate G is reciprocally proportional to the reciprocal half-crystallization time $t_{1/2}^{-1}$. Then it can be obtained [36]:

Table 3 The crystallization activation energy ΔE and surface free energy σ_e of PP and its composites

Sample	ΔE/kJ mol^{-1}	K_g (10^6 * K^{-2})	σ_e/J m^{-2}
PP	213.5	1.10	0.183
PP-10	268.3	0.86	0.143
PP-10a	298.3	0.71	0.118
PP-10b	266.6	0.84	0.140
PP-10c	240.5	0.94	0.157

$$\ln(t_{1/2})^{-1} + U^*/(R(T_c - T_\infty)) = \mathrm{A} - K_g/(T_c\Delta T f) \quad (3)$$

where U^* is the activation energy of polymer segments transporting to the crystal front through the subcooled melt, and U^* is 6270 J/mol for PP, R is the gas constant, T_∞ is the temperature somewhat below the glass transition temperature T_g and is given by $T_g - 30$ K (T_g is 263 K for PP), T_c is the crystallization temperature, ΔT is the degree of supercooling ($T_m^\circ - T_c$), where T_m° is the equilibrium melting temperature (here T_m° is 481 K for PP), f is a correcting factor for variation in the heat of fusion with temperature and is approximated by $f = 2T_c/(T_m^\circ + T_c)$, and K_g is the nucleation constant.

The plots of $\ln(t_{1/2})^{-1} + U^*/(R(T_c - T_\infty))$ against $1/(T_c\Delta T f)$ give a straight line (Fig. 8). The K_g values of specimens can be calculated form the slope of the line, tabulated in Table 3. The fold surface free energy σ_e can be obtained by the following equations [40]:

$$K_g = 4\sigma\sigma_e b_0 T_m^\circ/k\Delta H \quad (4)$$

$$\sigma = \alpha b_0 \Delta H \quad (5)$$

where k is the Boltzman constant, b_0 is the thickness of the molecular layer and is determined by lattice parameters (b_0 is 6.56×10^{-10} m), ΔH is the theoretical heat of fusion (ΔH is 1.4×10^8 J/m^3 for PP), σ and σ_e are interfacial free energies per unit area parallel and perpendicular to the

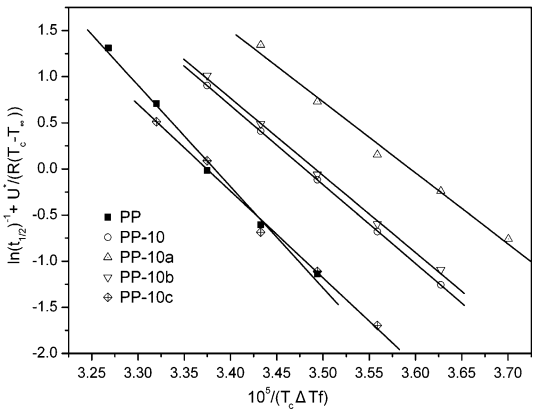

Fig. 8 The plot of $\ln(t_{1/2})^{-1} + U^*/(R(T_c - T_\infty))$ against $1/(T_c\Delta Tf)$ for PP and PP/nano-$CaCO_3$ composites with and without compatibilizers

molecular chain direction, respectively. The value of σ for PP is 9.2×10^{-3} J/m^2, so the fold surface free energy σ_e can be directly obtained from K_g is shown in Table 3. Generally, the smaller the σ_e of crystallization surface, the more easy the formation of nuclei is. It can be seen from Table 3 that addition of nano-$CaCO_3$ decreases the σ_e and addition PP-g-MA further decreases the σ_e. It is suggested that nano-$CaCO_3$ and the carboxylate salts formed by reaction between nano-$CaCO_3$ and compatibilizer can act as nucleating agents, reduce the free energy barrier for nucleation and increase the nucleation and crystallization rate of PP. However, the σ_e increases with decreasing the miscibility between compatibilizer and PP, indicating the poor miscibility between compatibilizer and PP does not favor the formation of nuclei.

Although addition of nano-$CaCO_3$ increases the ΔE of PP, the crystallization rate of PP is controlled by nucleation rate. The addition of nano-$CaCO_3$ and the formation of carboxylate salts acted as the heterogeneous nucleating agent favor the formation of nuclei. Therefore, the crystallization rate is increased in PP/nano-$CaCO_3$ composites due to the existence of large amounts of heterogeneous nuclei. However, the heterogeneous nucleation of nano-$CaCO_3$ and carboxylate salts depends on the miscibility between PP and compatibilizer. The decrease in the miscibility between compatibilizer and PP restricts the heterogeneous nucleation of nano-$CaCO_3$ and carboxylate salts, resulted in the low crystallization rate in PP/nano-$CaCO_3$ composites.

Conclusions

The crystallization and melting behavior of modified PP/nano-$CaCO_3$ composites with different interfacial interaction between compatibilizer and PP were investigated using differential scanning calorimetry, X-ray diffraction and polarized optical microscope. The results indicate addition of different compatibilizer has a different effect on the crystallization behavior of PP. The addition of PP-g-MA increases the crystallization temperature of PP. However, the crystallization temperature of PP is decreased by adding of POE-g-MA and EVA-g-MA. The addition of nano-$CaCO_3$ increases the crystallization temperature of PP due to the heterogeneous nucleation of nano-$CaCO_3$. The higher crystallization temperature of PP in modified PP/nano-$CaCO_3$ composite is attributed to the synergistic effect of heterogeneous nucleation of nano-$CaCO_3$ and compatibilizer due to the formation of carboxylate salts by the chemical reaction between the compatibilizers and nano-$CaCO_3$. The synergistic effect of heterogeneous nucleation of nano-$CaCO_3$ and compatibilizer further increases the crystallization temperature, crystallization rate and decreases the fold surface free energy as well as favors the formation of β-crystal of PP. However, the synergistic effect of heterogeneous nucleation of nano-$CaCO_3$ and compatibilizer for PP crystallization depends on the miscibility between PP and compatibilizer. The increased miscibility between compatibilizer and PP favors the synergistic effect of heterogeneous nucleation of nano-$CaCO_3$ and compatibilizer.

Acknowledgements The project was supported by Natural Science Foundation of China (Grant No. 50873115), Doctoral Fund of Ministry of Education of China and Project of Science and Technology of Guangdong Province, China (Grant No. 0711020600002).

References

1. Dagani R. Putting the 'nano' into composites. Chem Eng News. 1999;77:25–37.
2. Yang H, Zhang Q, Guo M, Wang C, Du RN, Fu Q. Study on the phase structures and toughening mechanism in PP/EPDM/SiO_2 ternary composites. Polymer. 2006;47:2106–15.
3. Zhang H, Zhang Z. Impact behaviour of polypropylene filled with multi-walled carbon nanotubes. Eur Polym J. 2007;43:3197–207.
4. Causin V, Marega C, Marigo A, Ferrara G, Ferraro A. Morphological and structural characterization of polypropylene/conductive graphite nanocomposites. Eur Polym J. 2006;42:3153–61.
5. Alexandre M, Dubois P. Polymer-layered silicate nanocomposites: preparation, properties and uses of a new class of materials. Mater Sci Eng. 2000;28:1–63.
6. Thridandapani RR, Mudaliar A, Yuan Q, Misra RDK. Near surface deformation associated with the scratch in polypropylene-clay nanocomposite: a microscopic study. Mater Sci Eng A. 2006;418:292–302.
7. Qin HL, Zhang SM, Zhao CG, Hu GJ, Yang MS. Flame retardant mechanism of polymer/clay nanocomposites based on polypropylene. Polymer. 2005;46:8386–95.
8. Lee HS, Fasulo PD, Rodgers WR, Paul DR. TPO based nanocomposites. Part 2. Thermal expansion behavior Polymer. 2006; 47:3528–39.
9. Ma CG, Mai YL, Rong MZ, Ruan WH, Zhang MQ. Phase structure and mechanical properties of ternary polypropylene/elastomer/nano-$CaCO_3$ composites. Compos Sci Technol. 2007; 67:2997–3005.

10. Thio YS, Argon AS, Cohen RE, Weinberg M. Toughening of isotactic polypropylene with $CaCO_3$ particles. Polymer. 2002;43:3661–74.
11. Zhang QX, Yu ZZ, Xie XL, Mai YW. Crystallization and impact energy of polypropylene/$CaCO_3$ nanocomposites with nonionic modifier. Polymer. 2004;45:5985–94.
12. Yang K, Yang Q, Li GX, Sun YJ, Feng DC. Mechanical properties and morphologies of polypropylene with different sizes of calcium carbonate particles. Polym Compos. 2006;27:443–50.
13. Weon JI, Gam KT, Boo WJ, Sue HJ. Impact-toughening mechanisms of calcium carbonate-reinforced polypropylene nanocomposite. J Appl Polym Sci. 2006;99:3070–6.
14. Chan CM, Wu JS, Li JX, Cheung YK. Polypropylene/calcium carbonate nanocomposites. Polymer. 2002;43:2981–92.
15. Zuiderduin WCJ, Westzaan C, Huetink J, Gaymans RJ. Toughening of polypropylene with calcium carbonate particles. Polymer. 2003;44:261–75.
16. Avella M, Cosco S, Di Lorenzo ML, Di Pace E, Errico ME, Gentile G. Nucleation activity of nanosized $CaCO_3$ on crystallization of isotactic polypropylene, in dependence on crystal modification, particle shape, and coating. Eur Polym J. 2006;42:1548–57.
17. Avella M, Cosco S, Di Lorenzo ML, Di Pace E, Errico ME. Influence of $CaCO_3$ nanoparticles shape on thermal and crystallization behavior of isotactic polypropylene based nanocomposites. J Therm Anal Calorim. 2005;80:131–6.
18. Lin ZD, Huang ZZ, Zhang Y, Mai KC, Zeng HM. Crystallization and melting behavior of nano-$CaCO_3$/polypropylene composites modified by acrylic acid. J Appl Polym Sci. 2004;91:2443–53.
19. Lin ZD, Zhang ZS, Huang ZZ, Mai KC. Investigation on preparation and property of nano-$CaCO_3$/PP masterbatch modified by reactive monomers. J Appl Polym Sci. 2006;101:3907–14.
20. Mai KC, Li ZJ, Zeng HM. Physical properties of PP-g-AA prepared by melt extrusion and its effects on mechanical properties of PP. J Appl Polym Sci. 2001;80:2609–16.
21. Ma CG, Rong MZ, Zhang MQ, Friedrich K. Irradiation-induced surface graft polymerization onto calcium carbonate nanoparticles and its toughening effects on polypropylene composites. Polym Eng Sci. 2005;45:529–38.
22. Wan WT, Yu DM, Xie YC, Guo XS, Zhou WD, Cao JP. Effects of nanoparticle treatment on the crystallization behavior and mechanical properties of polypropylene/calcium carbonate nanocomposites. J Appl Polym Sci. 2006;102:3480–88.
23. Shen H, Wang YH, Mai KC. Non-isothermal crystallization behavior of PP/$Mg(OH)_2$ composites modified by different compatibilizers. Thermochim Acta. 2007;457:27–34.
24. Causin V, Marega C, Saini R, Marigo A, Ferrara G. Crystallization behavior of isotactic polypropylene based nanocomposites. J Therm Anal Calorim. 2007;90:849–57.
25. Reyes-de Vaaben S, Aguilar A, Avalos F, Ramos-de Valle LF. Carbon nanoparticles as effective nucleating agents for polypropylene. J Therm Anal Calorim. 2008;93:947–52.
26. Lin ZD, Qiu YX, Mai KC. Crystallization and melt Behavior of $Mg(OH)_2$/PP composites modified by functionalized polypropylene. J Appl Polym Sci. 2004;92:3610–21.
27. Seo Y, Kim J, Kim KU, Kim YC. Study of the crystallization behaviors of polypropylene and maleic anhydride grafted polypropylene. Polymer. 2000;41:2639–46.
28. Gonzalez-Montiel A, Keskkula H, Paul DR. Morphology of nylon 6/polypropylene blends compatibilized with maleated polypropylene. J Polym Sci Polym Phys. 1995;33:1751–67.
29. Kawasumi M, Hasegawa N, Kato M, Usuki A, Okada A. Preparation and mechanical properties of polypropylene-clay hybrids. Macromolecules. 1997;30:6333–8.
30. McNally T, McShane P, Nally GM, Murphy WR, Cook M, Miller A. Rheology, phase morphology, mechanical, impact and thermal properties of polypropylene/metallocene catalysed ethylene 1-octene copolymer blends. Polymer. 2002;43:3785–93.
31. Huerta-Martínez BM, Ramírez-Vargas E, Medellín-Rodríguez FJ, Cedillo García R. Compatibility mechanisms between EVA and complex impact heterophasic PP-EPx copolymers as a function of EP content. Eur Polym J. 2005;41:519–25.
32. Di Lorenzo ML. Spherulite growth rates in binary polymer blends. Prog Polym Sci. 2003;28:663–89.
33. Tabtiang A, Venables R. The performance of selected unsaturated coatings for calcium carbonate filler in polypropylene. Eur Polym J. 2000;36:137–48.
34. Zhou WH, Lu M, Mai KC. Isothermal crystallization, melting behavior and crystalline morphology of syndiotactic polystyrene blends with highly-impact polystyrene. Polymer. 2007;48:3858–67.
35. Kissinger HE. Variation of peak temperature with heating rate in differential thermal analysis. J Res Natl Stand. 1956;57:217–21.
36. Zhang YF, Xin Z. Isothermal and nonisothermal crystallization kinetics of isotactic polypropylene nucleated with substituted aromatic heterocyclic phosphate salts. J Appl Polym Sci. 2006;101:3307–16.
37. Jang GS, Cho WJ, Ha CS. Crystallization behavior of polypropylene with or without sodium benzoate as a nucleating agent. J Polym Sci B: Polym Phys. 2001;39:1001–16.
38. Zhao SC, Cai Z, Xin Z. A highly active novel β-nucleating agent for isotactic polypropylene. Polymer. 2008;49:2745–54.
39. Hoffman JD. Regime III crystallization in melt-crystallized polymers: The variable cluster model of chain folding. Polymer. 1983;24:3–26.
40. Monasse B, Haudin JM. Growth transition and morphology change in polypropylene. Colloid Polym Sci. 1985;263:822–31.